

## MEASUREMENT OF $^3\text{He}/^4\text{He}$ IN THE LOCAL INTERSTELLAR MEDIUM: THE COLLISA EXPERIMENT ON *MIR*

E. SALERNO, F. BÜHLER, P. BOCHSLER, H. BUSEMANN, AND M. L. BASSI  
Physikalisches Institut, University of Bern, Silderstrasse 5, CH-3012 Bern, Switzerland

AND

G. N. ZASTENKER, YU. N. AGAFONOV, AND N. A. EISMONT  
Space Research Institute (IKI), Russian Academy of Sciences, Moscow, Russia

Received 2002 February 27; accepted 2002 November 19

### ABSTRACT

An accurate measurement of the noble gas isotopic composition in the local interstellar medium (LISM) provides a constraint of primary importance for modeling Galactic evolution and, in some cases, for studying the production of light nuclei in the early universe. The foil collection technique offers a direct way to measure some local interstellar gas abundances. With this method thin metal foils are exposed to the flux of neutral interstellar particles. Particles with sufficient energy penetrate the foil and remain trapped within its atomic structure. With the COLLISA experiment we have used this technique to collect a sample of interstellar neutral matter with the aim of determining the helium isotopic ratio in the LISM. The foils were exposed on board the Russian space station *Mir*. After exposure in space, the foils were brought back to the Earth, and the amount of captured particles was determined by mass spectrometric analysis at the University of Bern. The analysis has allowed the detection of interstellar  $^3\text{He}$  and  $^4\text{He}$  and the determination of the LISM isotopic number ratio  $^3\text{He}/^4\text{He} = (1.7 \pm 0.8) \times 10^{-4}$ . This value is consistent with protosolar ratios obtained from meteorites and Jupiter's atmosphere, supporting the hypothesis that negligible changes of the abundance of  $^3\text{He}$  occurred in the Galaxy during the past 4.5 Gyr.

*Subject headings:* Galaxy: abundances — Galaxy: evolution — ISM: abundances —  
ISM: individual (local interstellar medium) — space vehicles

### 1. INTRODUCTION

High-precision studies of the helium abundance and isotopic composition in different locations of the Galaxy have great importance for cosmology and for stellar and Galactic evolution. According to the standard big bang model of nucleosynthesis (SBBN), helium was synthesized during the first few minutes after the big bang together with the other light nuclei D and  $^7\text{Li}$ . At that time the abundances relative to hydrogen ranged from  $\sim 10^{-10}$  (for lithium), to  $\sim 10^{-5}$  (for deuterium and  $^3\text{He}$ ), and to  $\sim 10^{-1}$  (for  $^4\text{He}$ ) (Steigman 1994). As a result of nucleosynthetic processes in the Galaxy, light-element abundances evolve secularly, and currently observed abundances in the interstellar medium differ from the primordial values. For instance, D is converted into  $^3\text{He}$  already during the pre-main-sequence phase in stars of all masses (Palla & Stahler 1991, 1993). In conventional models  $^3\text{He}$  is partially transformed into  $^4\text{He}$  in stellar interiors. Some unprocessed  $^3\text{He}$  from the outer convective zone of low-mass stars is returned to the interstellar medium after the star's death. However, the fraction of low-mass stars following this evolutionary track might be as low as a few percent, whereas all other low-mass stars undergo “cool bottom processing,” thereby destroying the remainders of  $^3\text{He}$  (the “ $^3\text{He}$  problem”) (see, e.g., Rood et al. 1998; Charbonnel 1995, 1998; Galli et al. 1995, 1997, and references therein). The aim of Galactic chemical evolution (or GCE) models is to reproduce these processes and predict the primordial value of the abundances using the observations as input parameters (Olive, Steigman, & Walker 2000). The determination of the primordial light-element abundances then allows SBBN models to set limits on the

baryon density of the universe, since the amount of nuclides produced primordially depends on the density of nucleons and on the early-universe expansion rate (Schramm & Turner 1998; Sakar 1996). A comparison of predicted abundances with those inferred from observational data is a key test to verify the validity of both GCE and SBBN models.

So far, considerable effort has been invested in improving the quality and the precision of measurements of light nuclides in different astrophysical sites. Among others, some experiments have been carried out to determine the kinematic properties and the distribution of helium in the local interstellar medium (LISM). Past studies on resonant backscattering of the solar extreme-ultraviolet radiation (Chassefière et al. 1986, 1988) allowed the study of some characteristic parameters of  $^4\text{He}$  neutral atoms of interstellar origin far from the Sun. Later Witte, Banaszkiewicz, & Rosenbauer (1996) determined velocity, direction, temperature, and density of the flow of interstellar helium from the measurements of the *Ulysses*/GAS experiment. Similarly, Gloeckler & Geiss (1998), using data from the SWICS mass spectrometer on the *Ulysses* spacecraft, derived the  $^3\text{He}/^4\text{He}$  ratio in the LISM from pickup helium measured in the high-speed solar wind. The determination of the isotopic composition of the LISM with this method is difficult because of the very low abundance of  $^3\text{He}$  pickup ions.

An independent way of determining the helium isotopic ratio consists of deriving it from direct observations of interstellar neutral atoms. Neutral gas of the LISM, reaching the Earth's orbit before interacting with the solar EUV photons, keeps the original isotopic abundance ratios and therefore represents a reliable sample for the study of interstellar matter.

In this paper we present the value of the isotopic ratio  $^3\text{He}/^4\text{He}$  measured in a sample of local interstellar neutral medium as collected with the COLLISA (Collection of Interstellar Atoms) experiment on *Mir*. In § 2 a description of the COLLISA project and the experimental method is given. In particular, the conditions necessary to trap neutral atoms from the LISM are defined. In § 4 we describe some physical properties of the copper-beryllium foils, used for the collection of interstellar particles, and we discuss the behavior of low-energy helium particles in BeO. The capture and release of helium as a function of the implantation energy and the foil temperature, respectively, are studied. Trapping efficiency and diffusion properties of helium in beryllium oxide are determined from measurements. Sections 3 and 5 report on data collection and data analysis, respectively. In § 6 we present the results of the mass spectrometric analysis, performed so far only on one of the exposed foils. Absolute amounts of  $^3\text{He}$  and  $^4\text{He}$  released from the foil are given, together with the corresponding LISM isotopic ratio. We then compare this ratio with protosolar and present-day values inferred from observations of other astrophysical sites. We also compare the accumulated  $^4\text{He}$  flux derived from COLLISA foils with the values obtained from other experiments and the values predicted from theoretical models of the flow of interstellar neutral helium inside the heliosphere up to 1 AU. Finally, we discuss possible implications of the newly determined helium isotopic ratio for some Galactic chemical evolution models.

## 2. THE EXPERIMENT

COLLISA is the result of a cooperation between the Space Research and Planetary Sciences Division of the University of Bern and the Space Research Institute (IKI) of the Russian Academy of Sciences. The experiment basically consists of collecting a sample of neutral atoms from the LISM with a metal foil exposed in space with the aim of measuring abundances and the isotopic composition of elements with high ionization potentials, e.g.,  $^3\text{He}/^4\text{He}$ ,  $^{20}\text{Ne}/^{22}\text{Ne}$ , and  $^4\text{He}/^{20}\text{Ne}$ . The experimental procedure is based on the “foil collection technique,” a method developed at the Physikalisches Institut of the University of Bern and successfully applied during the *Apollo* missions to collect solar wind ions on the surface of the Moon (Geiss et al.

1970, 1972; Bühler et al. 2000). If the kinetic energy of the particles is sufficient (typically  $20 \text{ eV amu}^{-1}$ , i.e.,  $60 \text{ eV}$  for  $^3\text{He}$ ), a fraction of them is trapped in the atomic structure of the foils. Within the framework of the COLLISA experiment, four copper-beryllium foils were mounted in two collectors placed on the outside of the module Spektr of the Russian space station *Mir*. The foils were exposed to the flux of interstellar neutral atoms for an integrated exposure time of  $\sim 60 \text{ hr}$ .

Neutral atoms of the LISM can cross the heliopause; they enter the heliosphere with a velocity of  $\sim 25 \text{ km s}^{-1}$ . Close to the Sun, photoionization and charge exchange with solar wind ions reduces the flux of neutrals. It may change the relative elemental abundances, but the isotopic composition of the ambient neutrals remains essentially unchanged. The Earth intercepts the stream of particles with a collision angle and an impact velocity that undergo seasonal changes (Fig. 1).

From January to May the orbital motion of the Earth is directed against the interstellar flux (from position A toward position B in Fig. 1). This condition, combined with the pull of solar gravity, produces a variability of the velocity of the neutral atoms relative to the Earth ranging from  $\sim 80$  to  $\sim 60 \text{ km s}^{-1}$ . The maximum relative speed corresponds to particle energies of the order of  $\sim 25 \text{ eV amu}^{-1}$ , sufficient to guarantee the capture of a sizeable fraction within the foils.

After exposure, the foils were recovered by the *Mir* cosmonauts and delivered to the Earth with the American Space Shuttle *Atlantis*.

## 3. COLLECTION OF INTERSTELLAR PARTICLES

Studies on the scattering of interstellar helium in the Earth’s atmosphere indicate that this process does not affect the foil collection of interstellar neutral atoms if the foils are exposed during minimum solar activity and at altitudes higher than  $300 \text{ km}$  (Bassi 1997). The Russian space station *Mir*, orbiting the Earth at a distance of  $\sim 400 \text{ km}$ , was therefore a suitable platform for the exposure of trapping foils. The exposure devices for the COLLISA experiment, named KOMZA I and II (Russian acronym for “collector of interstellar atoms”), were designed and built at IKI with the participation of the Space Physics Design Bureau (Zastenker

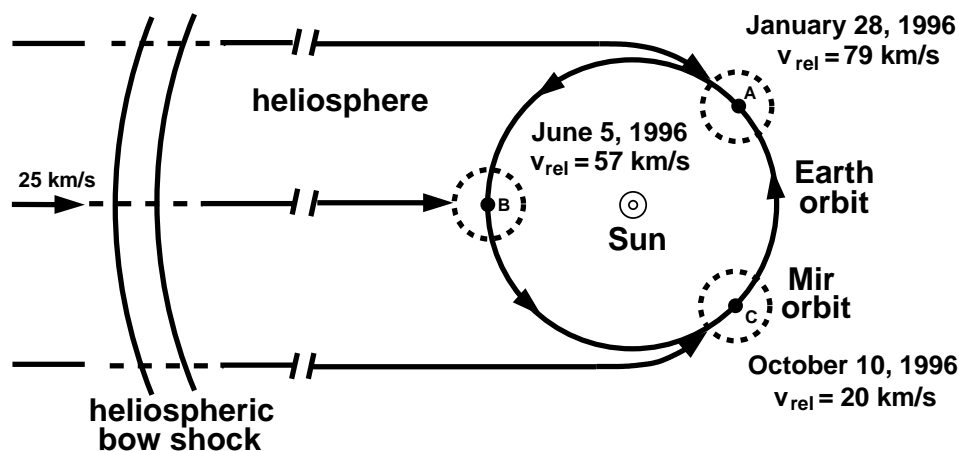


FIG. 1.—Seasonal variation of speed and direction of the interstellar flux of neutrals. From January to May the velocity of the interstellar particles relative to the Earth decreases from  $80$  to  $60 \text{ km s}^{-1}$ .

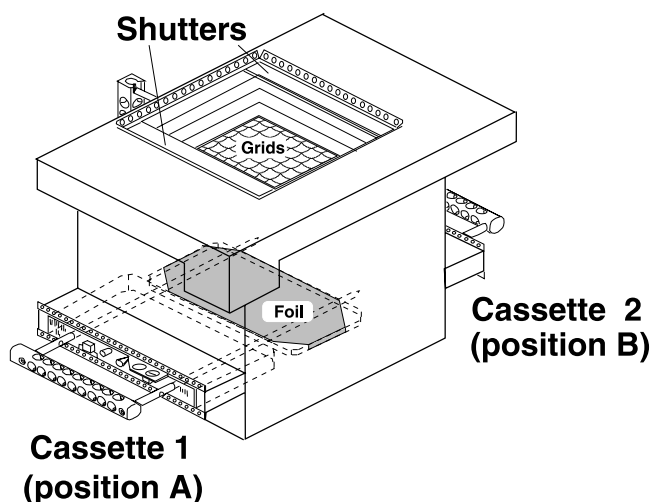


FIG. 2.—Schematic drawing of a KOMZA collector. Only one of the two cassettes is shown in detail.

et al. 2002). Both exposure devices were mounted outside the Spektr module and launched and docked to *Mir* in 1995 May together with this module.

The KOMZA exposure device (Fig. 2) basically consists of a collector box with an opening at the top. The stream of interstellar particles flowing through the apertures is trapped in foils at the base of the collector box. Special replaceable cassettes (Fig. 2, *dashed lines*), plugged into the collector, were used as foil-protecting support. Both KOMZA apertures were provided with shutters, which were opened only when the best exposure conditions prevailed. Utmost care was taken to keep the shutters closed to prevent any occasion of possible contamination of the foils with atmospheric particles during unfavorable attitudes of the space station. The shutters were also closed during docking, undocking, refuelling, and activation of cruise or attitude control engines of *Mir*. Although the optimization of the exposure conditions, as described above, significantly reduced risks of many possible interferences, it limited the total exposure period to approximately 60 hr, which is much less than could have been achieved with an experiment on an unmanned, remotely controlled spacecraft. Contamination of the foils with condensables from the manned spacecraft were of serious concern since SRIM (stopping and range of ions in matter) simulations had indicated earlier that the implantation of helium atoms can be strongly reduced if layers of condensed molecules cover the foils. In order to check possible modifications of the trapping efficiency of our foils during exposure, some small foil samples, exposed in space, were artificially bombarded in the laboratory with helium particles at nominal interstellar energies a few months after the exposure in space.

To minimize risks of contamination, heating plates were placed just below the foils of KOMZA II to keep them at a temperature of 55°C. This measure should inhibit the formation of condensation layers, which could prevent low-energy interstellar particles from being trapped. Another measure of precaution consisted in checking the foils for possible diffusion losses at the given thermal conditions during exposure: preirradiated witness pieces (irradiated with  ${}^3\text{He}$  at 25 eV  $\text{amu}^{-1}$ ) were mounted next to the collector

foils, thus enabling checks of storage conditions and possible helium losses that could have occurred between launch and recovery of the foils. As a measure against possible irradiation with energetic magnetospheric ions, electrical grids had been placed into the collectors above the foils in order to reject positively charged ions with energies up to 5 keV  $q^{-1}$ .

As indicated in § 2, the optimum season for exposure in the orbit of the Earth lasts from January to May. Consequently the shutters were opened from 1996 January 15 to May 23 for several minutes per day, and four 200  $\text{cm}^2$  foil pieces were exposed to the flux of the interstellar neutrals. 1996 was a particularly favorable year because solar activity had reached its minimum, thus minimizing the effect of interstellar particles being scattered by exospheric particles.

#### 4. FOIL PROPERTIES

For the COLLISA experiment we have used commercial copper-beryllium foils (2% of Be by mass), approximately 15  $\mu\text{m}$  thick. A first plasma cleaning treatment was applied to the foils to remove discoloration caused by oxidation. The foils were then flushed at 600°C for  $\sim 3$  hr in tritium-poor water (1 bar) to reduce the  ${}^3\text{H}$  background and thus to prevent the production of  ${}^3\text{He}$  from  ${}^3\text{H}$  decay in the bulk of the metal. Finally, a 20 nm thick, smooth, and homogeneous BeO surface layer was generated by heating the foils for 20 minutes to 680°C in a low-pressure, tritium-poor water vapor (Jordi 1982). The treatment with tritium-poor hydrogen was necessary because investigations (Jordi 1986) of noble gases contained in freshly produced foils had revealed large concentrations of  ${}^3\text{He}$  ( $\sim 2 \times 10^5$  atoms  $\text{cm}^{-2}$ ). This high  ${}^3\text{He}$  background content was attributed to the decay of tritium inside the BeO layer. An ubiquitous tritium contamination of materials due to nuclear tests, which peaked between 1962 and 1965, has caused difficulties for many disciplines in the environmental sciences for four decades. Although the amount of tritium contained in the foils is too low to be detected through its radioactive decay with conventional means,  ${}^3\text{He}$  resulting from decay could interfere with the detection of the interstellar atoms.

##### 4.1. Trapping Efficiency

Filleux et al. (1980) investigated the “trapping efficiency” of different metal targets for helium isotopes as a function of particle kinetic energy. The trapping efficiency  $\eta$  of a given target is defined as the percentage of particles captured by the target compared to the total irradiated amount. Optimum trapping efficiencies were obtained using copper-beryllium foils with a thin surface film of beryllium oxide. At energies larger than 500 eV no significant difference between the trapping of  ${}^3\text{He}$  and  ${}^4\text{He}$  was observed within the limits of experimental accuracy (1  $\sigma$  corresponding to  $\pm 5\%$  uncertainty). In the low-energy range a strong dependence of  $\eta$  upon the incoming ion energy was found in all types of metal targets (Fig. 3).

An extensive series of test measurements was performed after the foil treatment in order to determine with enhanced accuracy the difference between the trapping efficiencies of  ${}^3\text{He}$  and of  ${}^4\text{He}$  at low energies ( $\sim 25$  eV  $\text{amu}^{-1}$ ). The foils used for the COLLISA experiment were bombarded in the CASYMS facility of the University of Bern (Ghielmetti et al. 1983). Average trapping efficiencies  $\bar{\eta} = 0.18 \pm 0.04$  and

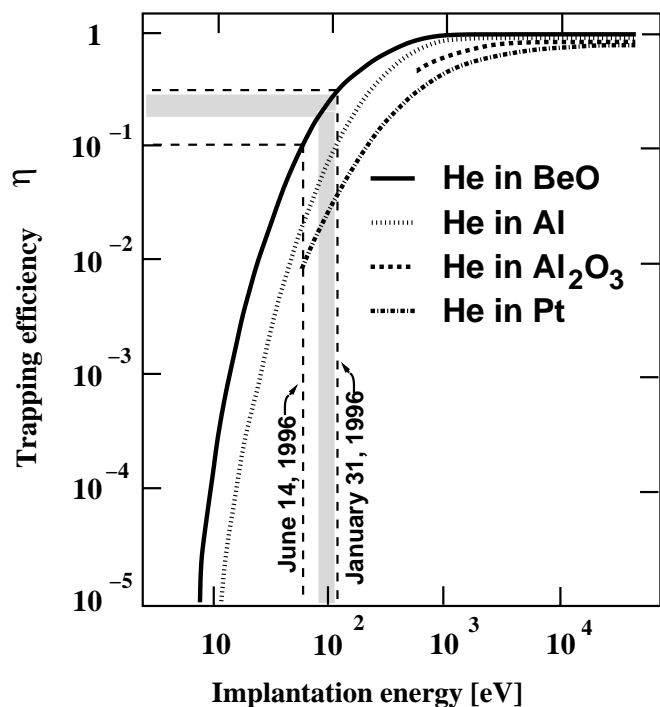


FIG. 3.—Trapping of He ions in polycrystalline Al and Pt, in BeO, and in anodic  $\text{Al}_2\text{O}_3$  films as a function of ion energy. Data from Filleux et al. (1980). Dashed vertical lines indicate the range of energies corresponding to the expected interstellar neutral energies near the Earth in the period from 1996 January 31 through June 14. The shaded area corresponds to the exposure period from 1996 January 16 through May 23. The maximum trapping efficiency ( $\sim 34\%$ ) is achieved at the end of January, when the relative velocity reaches  $79.5 \text{ km s}^{-1}$  ( $\sim 33 \text{ eV amu}^{-1}$ ). By June 14 the relative velocity drops to  $54 \text{ km s}^{-1}$  ( $\sim 15 \text{ eV amu}^{-1}$ ), corresponding to a trapping efficiency of  $\sim 10\%$ .

$\bar{\eta}_4 = 0.24 \pm 0.04$  were found. The corresponding trapping ratio  $\eta_3/\eta_4$  shows a flat distribution with an average of 0.73 and a standard deviation of 0.07 (Fig. 4).

As discussed above, some samples of foils, which had previously been exposed on *Mir*, have been artificially bombarded after flight to check whether the trapping efficiency was modified during space exposure. Indeed, for both species,  $^3\text{He}$  and  $^4\text{He}$ , a systematic reduction of trapping efficiencies by as much as a factor of 2 had occurred during the exposure in space (see Table 1).

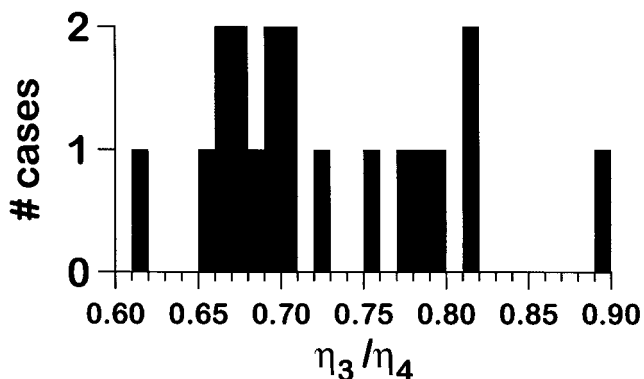


FIG. 4.—Distribution of the ratio of the trapping efficiencies. Data from Bassi (1997).

TABLE 1  
TRAPPING EFFICIENCIES OF UNFLOWN AND FLOWN FOILS

SPECIES AND IMPLANTATION ENERGY	L431		L461	
	Unflown	Flown	Unflown	Flown
$^3\text{He}$ 75 eV .....	0.18	0.08	0.21	0.10
$^4\text{He}$ 100 eV .....	0.24	$\sim 0.09$	0.28	$\sim 0.12$
	0.22			

This deterioration is tentatively attributed to a surface layer of contaminants that built up during exposure. It has to be taken into account for an inference of the absolute helium density in the LISM (§ 7.1). However, while the trapping efficiencies both for  $^3\text{He}$  and for  $^4\text{He}$  decreased during exposure, their ratio remained approximately constant, as can be derived from Table 1. To account for systematic uncertainties in the calibration process, as well as for the possibility that the ratio between the trapping efficiencies for  $^3\text{He}$  and for  $^4\text{He}$  could have increased somewhat during exposure, we expand the error for this ratio and shall assume in the following:  $\eta_3/\eta_4 = 0.73^{+0.10}_{-0.13}$ . Even so, any modification of the ratio of the trapping efficiencies during exposure obviously will not hamper the determination of the isotopic ratio of LISM helium (see § 6.3).

#### 4.2. Diffusion of He in BeO

Whether a particle is trapped in a solid depends upon its ability to convey a significant part of its momentum to the surface grid atoms of the solid, to damage the grid, and on its ability thus to penetrate through the first few atomic layers. Considering the further fate of these atoms after an artificial or interstellar bombardment, we expect that, at the energies under consideration, particles are decelerated over distances of a few nanometers and perform some random walk while diffusing inside the solid medium. While both species,  $^3\text{He}$  and  $^4\text{He}$ , decelerate over very similar distances, the lighter isotope has a noticeably longer diffusion mean free path, leading to more substantial losses and to a lower trapping efficiency. Numerical simulations using the SRIM code (Ziegler, Biersack, & Littmark 1985) in fact indicate that both He nuclides implanted at typical energies of interstellar neutrals accumulate within a relatively narrow layer about 2–3 nm below the surface (Fig. 5).

Given the low irradiation doses and the low energies of the impacting particles, no significant temperature enhancement is expected to occur in the foil during irradiation, and, as will be discussed below, implanted helium will remain within the foils for years as long as the foil temperature remains below  $200^\circ\text{C}$ . Considering the fact that particles with significantly different implantation energies rest at different depths in the foil, diffusion properties can be exploited with the stepwise heating method during noble gas analysis to distinguish atoms from different origins and to obtain indirect information on the implantation energy. Stepwise heating extraction, performed on different CuBe foils, which had been artificially bombarded with He ions in monoenergetic beams at different energies, demonstrated that there is indeed a relation between the kinetic energy of the injected atoms and their release temperature. Particles implanted in the foils with typical interstellar energies are preferentially released in a temperature range of

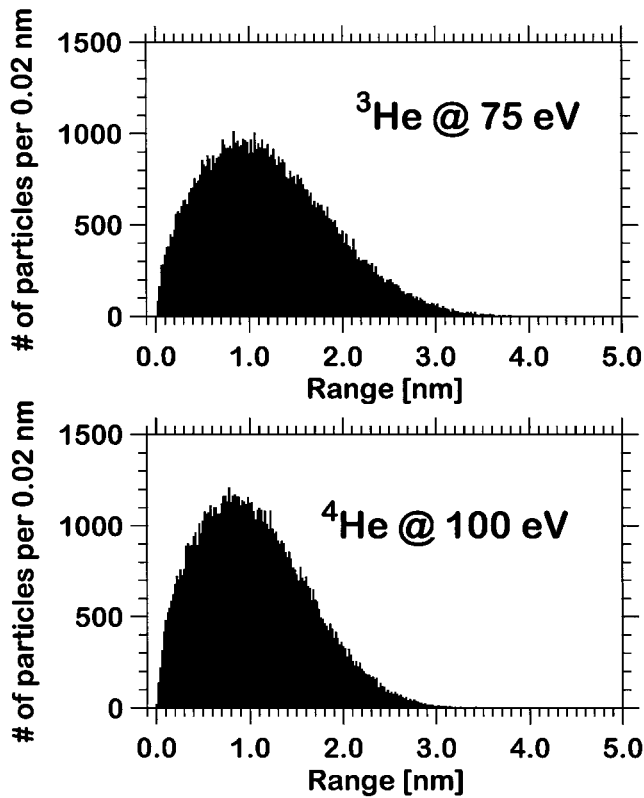


Fig. 5.—Illustration of the range distribution of helium particles in BeO simulated with the SRIM package (Ziegler et al. 1985). The figure shows the depth distribution of He atoms in a BeO target (50% Be and 50% O, density  $3 \text{ g cm}^{-3}$ ) implanted with  $25 \text{ eV amu}^{-1}$ .

$600^\circ\text{C}$ – $1100^\circ\text{C}$ , whereas particles implanted with significantly lower and significantly higher energies are released below  $600^\circ\text{C}$  and above  $1100^\circ\text{C}$ , respectively (Table 2).

## 5. MASS SPECTROMETRIC ANALYSIS

### 5.1. The Samples

The analysis was performed on one of the foils exposed on the collector KOMZA II. A sample of  $137 \text{ cm}^2$ , labeled L461-2-1, was cut from the foil and subdivided into three stripes that were tightly rolled together and packed into nickel foil containers.

Three samples of preirradiated witness pieces, each of  $2.8 \text{ cm}^2$ , were introduced separately into nickel containers. Three additional samples, L461-3-2, L460-3-1, and L461-3-5, which had never been flown in space were analyzed for

TABLE 2  
IMPLANTATION ENERGY AND RELEASE TEMPERATURE

Experimental Implantation Energy	Temperature Range Suitable for Extraction ( $^\circ\text{C}$ )	Possible Source of Implanted Helium
$15 \text{ eV amu}^{-1}$ ....	300–600	Atmospheric ( $\sim 1 \text{ eV}$ )
$25 \text{ eV amu}^{-1}$ ....	600–1100	Interstellar ( $10$ – $100 \text{ eV}$ )
$5000 \text{ eV}$ .....	1100–1700	Magnetospheric ( $10^3$ – $10^6 \text{ eV}$ )

NOTE.—Data are based on measurements performed on CuBe foils artificially bombarded with He isotopes at  $15 \text{ eV amu}^{-1}$ , at  $25 \text{ eV amu}^{-1}$ , and at  $5000 \text{ eV}$ . For comparison, possible origins of particles are identified in the third column.

“foil blank” (see § 5.3). The samples had areas of  $125$ ,  $141$ , and  $135 \text{ cm}^2$ , respectively.

### 5.2. Gas Extraction and Analysis

Samples were routinely heated in temperature steps of  $300^\circ\text{C}$ ,  $600^\circ\text{C}$ ,  $1100^\circ\text{C}$ ,  $1400^\circ\text{C}$ , and  $1700^\circ\text{C}$  in a closed ultrahigh vacuum system at pressures at or below  $10^{-8}$  mbar. Helium was extracted from the samples, and after thorough cleaning from chemically active gases and impurities over hot metal getters and cooled activated charcoal, it was transferred into a mass spectrometer for the isotope analysis.

### 5.3. Blanks

In order to determine the experimental background, several measurements of the noble gases contained in the empty analysis system at room temperature were performed. The helium cold blank values were on average  ${}^3\text{He} = (6.8 \pm 3.2) \times 10^5$  and  ${}^4\text{He} = (6.2 \pm 1.6) \times 10^9$  atoms.

A series of measurements of empty nickel containers was also performed with the stepwise heating to monitor the gas release from the hot extraction system (“extraction blanks”). At elevated temperatures the  ${}^3\text{He}$  extraction blanks turned out to be comparable to the cold blank values. At  $1100^\circ\text{C}$  a slightly higher amount of  ${}^4\text{He}$ ,  $(1.1 \pm 0.2) \times 10^{10}$  atoms, was detected.

The so-called foil blanks were determined using three foils never flown in space. For  ${}^4\text{He}$  no significant difference was found between extraction blanks and foil blanks at the corresponding temperatures. However, a non-negligible amount of  ${}^3\text{He}$  was registered at  $1100^\circ\text{C}$ . The maximum amount released from the blank foils (after subtraction of the extraction blank) at  $1100^\circ\text{C}$  was  ${}^3\text{He} = (1.4 \pm 0.2) \times 10^7$  and  ${}^4\text{He} = (3.4 \pm 2.4) \times 10^9$  atoms.

As indicated in § 4.1, we must attribute the  ${}^3\text{He}$  background to the in situ decay of tritium contained in the foil. The comparison between the current foil blank values and those derived from measurements of foils not pretreated with  $600^\circ\text{C}$  tritium-poor hydrogen (see § 4) showed that the special treatment improved the  ${}^3\text{He}$  foil background somewhat, but unfortunately it did not eliminate it.

## 6. RESULTS

### 6.1. Release Curves from Stepwise Extraction

Figure 6 illustrates the results of the analysis performed on the foil L461-2-1 exposed to interstellar particles.

The continuous lines show the cumulated amount of  ${}^3\text{He}$  and  ${}^4\text{He}$  (*upper and lower panels, respectively*) released per  $\text{cm}^2$  foil at the given temperature step. For comparison, data derived from the analysis of the blank foils L461-3-2, L460-3-1, and L461-3-5 (*dashed lines*) are also plotted. Tables 3 and 4 show the (differential) releases for each temperature step, uncorrected for any background. Given errors are experimental and are derived from the scatter of the individual data points. The results for  ${}^4\text{He}$  show that there is no serious difficulty distinguishing the interstellar component from the foil blank. The exposed foil released the largest amount of gas in the temperature step of  $1100^\circ\text{C}$ , as expected for particles with interstellar energies (see Table 2). The interpretation of the  ${}^3\text{He}$  release curves is more difficult

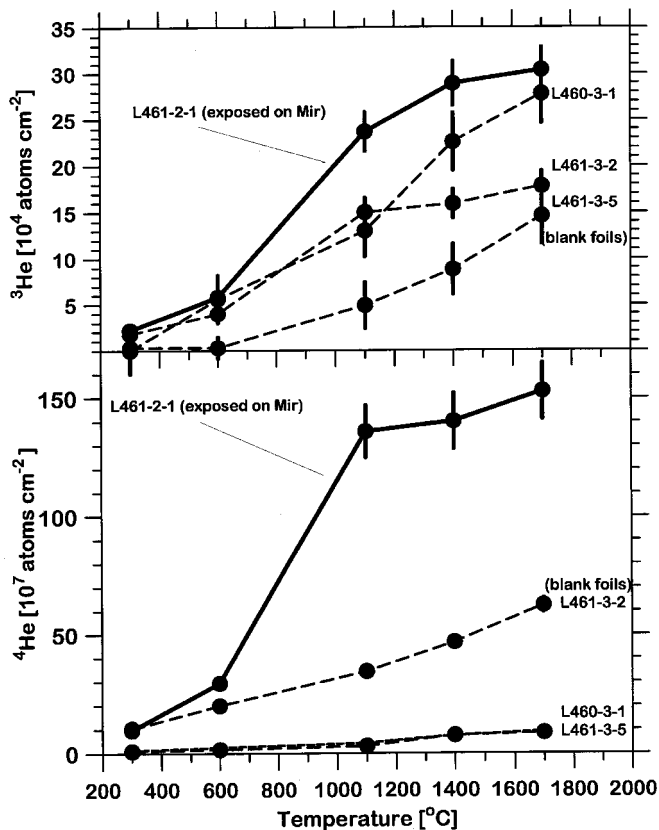


FIG. 6.—Accumulated stepwise release of <sup>3</sup>He and <sup>4</sup>He, uncorrected. Continuous lines show the helium released from an exposed foil. Dashed lines illustrates the stepwise yields of unflown foils.

since the foil blanks are of the same order of magnitude as the amount attributed to interstellar origin. Nevertheless, in all three cases the average number of <sup>3</sup>He atoms released from the blank foils up to 1100°C is significantly below the value for the flown foil at the given temperature step.

6.2. Modeling of Release Curves

To check the consistency of our interpretation, we set up a simple diffusion model, assuming that the parameters describing the diffusion of helium out of the surface layers follow an Arrhenius law,

$$D(T) = D_0 e^{-Q/kT}.$$

We use the observed release profile of <sup>4</sup>He, which we interpret as a surface-implanted component, to derive the parameters  $D_0$  and  $Q$  (the activation energy for the diffusion

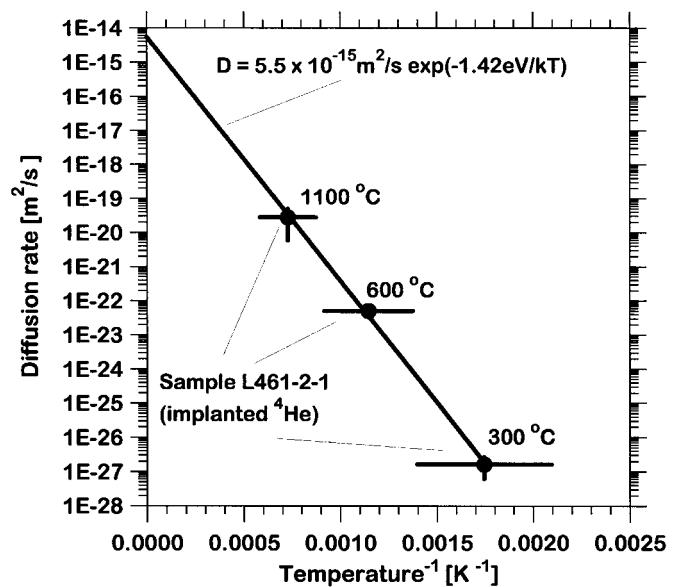


FIG. 7.—Arrhenius plot derived from the <sup>4</sup>He temperature release curve of sample L461-2-1 assuming an initial rectangular profile of 2 nm depth. From the slope of the straight line, the activation energy for diffusion is derived. The intercept at  $1/T \rightarrow 0$  gives the diffusion parameter  $D_0$ .

process). Assuming a 2 nm wide rectangular initial concentration profile within the BeO layer, we derive from the first three temperature steps a diffusion parameter  $D_0 = 5.5 \times 10^{-15} \text{ m}^2 \text{ s}^{-1}$  and an activation energy  $Q = 1.42 \text{ eV atom}^{-1}$ . The procedure is illustrated in the Arrhenius diagram in Figure 7.

Using the parameters derived above, the release curve of a volume-concentrated helium component (e.g., <sup>3</sup>He from tritium decay), which is homogeneously distributed in a 20 nm deep BeO layer, can be modeled. The result is shown in Figure 8. The agreement of the modeled curves with the observed release curves (Fig. 6) supports the assumption that the stepwise extraction technique allows the separation of surface-implanted components from components distributed homogeneously throughout the BeO layer. Whereas <sup>4</sup>He is contained only in a narrow surface layer, <sup>3</sup>He apparently sits deep in the foils. Furthermore, the diffusion parameters derived above allow an extrapolation of the diffusion properties of helium within BeO at lower temperatures: Adopting the parameters given above and assuming a foil temperature of less than 200°C, it would take at least 100 yr for a helium atom to migrate through one monolayer of BeO. Thus, once a helium atom is captured within a foil, diffusion losses at normal storage temperatures are negligible.

TABLE 3  
TRAPPED <sup>3</sup>He

$T$ (°C)	L461-2-1 (exposed) (10 <sup>4</sup> atoms cm <sup>-2</sup> )	L461-3-2 (blank) (10 <sup>4</sup> atoms cm <sup>-2</sup> )	L460-3-1 (blank) (10 <sup>4</sup> atoms cm <sup>-2</sup> )	L461-3-5 (blank) (10 <sup>4</sup> atoms cm <sup>-2</sup> )
300	2.2 ± 0.5	1.8 ± 0.4	0.0 ± 2.5	0.3 ± 0.3
600	3.6 ± 0.4	2.2 ± 0.5	5.6 ± 0.7	0.0 ± 1.1
1100	17.9 ± 2.0	11.0 ± 1.4	7.4 ± 1.0	4.6 ± 1.1
1400	5.2 ± 1.1	0.9 ± 0.2	9.6 ± 1.4	3.9 ± 1.1
1700	1.5 ± 0.4	1.9 ± 0.4	5.2 ± 0.6	5.8 ± 1.3

TABLE 4  
 TRAPPED  $^4\text{He}$ 

$T$ ( $^{\circ}\text{C}$ )	L461-2-1 (exposed) ( $10^7$ atoms $\text{cm}^{-2}$ )	L461-3-2 (blank) ( $10^7$ atoms $\text{cm}^{-2}$ )	L460-3-1 (blank) ( $10^7$ atoms $\text{cm}^{-2}$ )	L461-3-5 (blank) ( $10^7$ atoms $\text{cm}^{-2}$ )
300.....	$9.6 \pm 1.0$	$10.3 \pm 1.0$	$1.1 \pm 0.1$	$0.8 \pm 0.1$
600.....	$19.8 \pm 2.0$	$9.6 \pm 1.0$	$1.3 \pm 0.1$	$0.7 \pm 0.1$
1100.....	$106.4 \pm 10.7$	$14.5 \pm 1.5$	$1.9 \pm 0.2$	$1.5 \pm 0.2$
1400.....	$4.3 \pm 4.3$	$12.3 \pm 1.2$	$3.0 \pm 0.3$	$4.4 \pm 0.3$
1700.....	$12.7 \pm 1.3$	$15.6 \pm 1.6$	$1.9 \pm 0.2$	$1.1 \pm 0.1$

### 6.3. Isotopic Ratio of Trapped Interstellar Helium

For the derivation of the isotopic ratio of trapped interstellar helium, the gas released at all temperature steps up to  $1100^{\circ}\text{C}$  (the nominal melting temperature of Cu) was cumulated. To correct for a possible contamination with  $^3\text{He}$ , the average  $^3\text{He}$  from the foil blanks in Table 3 was subtracted from the  $^3\text{He}$  released by the exposed foil L461-2-1. (The values in Tables 3 and 4 are uncorrected for any background.) For  $^4\text{He}$ , the L461-3-2 blank value is the appropriate correction to be applied to the value for the exposed foil L461-2-1, in place of an average of the three blanks given in Table 4. The foils L460-3-1 and L461-3-5 were measured in a later series of analyses for which the  $^4\text{He}$  extraction blank was improved. The three foil blanks are thus representative for the  $^3\text{He}$  blank but not for  $^4\text{He}$ . The isotopic ratio of helium captured in the foil is thus  $^3\text{He}/^4\text{He} = (1.22 \pm 0.56) \times 10^{-4}$ . Error bars are estimated in a conservative manner in order to take into consideration the low number of the blank foils analyzed so far. The analysis of the witness pieces, the results of which are not shown in Figure 6, confirmed that no significant loss of particles occurred during flight.

After correction for isotopic bias introduced with the different trapping efficiencies for different species,  $\eta_3/\eta_4 = 0.73^{+0.10}_{-0.13}$ , a ratio of

$$^3\text{He}/^4\text{He} = (1.7 \pm 0.8) \times 10^{-4}$$

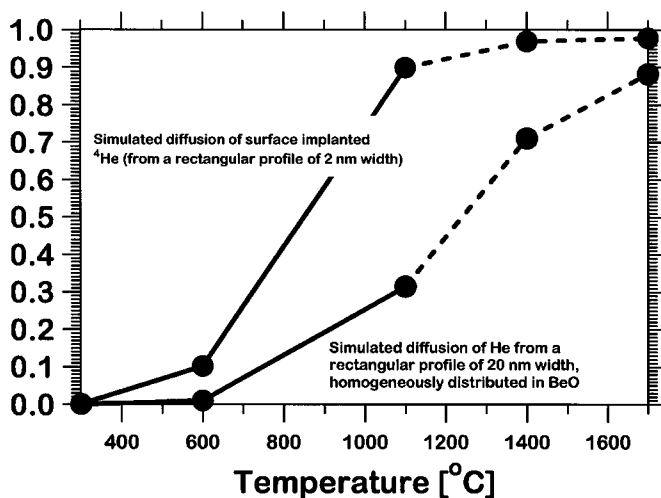


FIG. 8.—Comparison of modeled release pattern. Three extraction steps at  $300^{\circ}\text{C}$ ,  $600^{\circ}\text{C}$ , and  $1100^{\circ}\text{C}$  allow the distinction between surface-implanted helium and helium rooted in deeper layers.

is derived for the helium isotopic abundance ratio of interstellar neutrals penetrating into the inner heliosphere.

## 7. DISCUSSION

### 7.1. Estimate of the Interstellar Neutral Helium Density

The flux of interstellar helium collected by a device such as the COLLISA experiment is determined by the flux penetrating the boundaries of the heliosphere. Hence, knowledge of all processes modifying the neutral flux within the heliosphere makes it possible to determine the interstellar flux of helium with COLLISA, and, since the velocity of the heliosphere relative to the surrounding interstellar medium is well known, the interstellar helium density outside the heliosphere can also be determined. However, an exact determination rests on an accurate knowledge of all factors that might modify the flux of particles between their entry into the heliosphere and their arrival at the COLLISA foils, including the velocity-dependent trapping efficiencies. Furthermore, the attitude of the space platform has to be known at every instant of exposure in order to determine the shadowing due to the collector walls.

Bassi (1997) carefully modeled the collected flux in COLLISA, assuming a thermal distribution of neutral particles at infinity in the interstellar medium. He took into account the seasonal variability of the local ionization efficiency by solar EUV due to the orbital motion of the Earth and the concomitant variability of the trapping efficiency of foils due to the seasonal variability of the relative velocity. A summary of the most relevant effects is outlined in Figure 9. From the decrease of the relative velocities of neutrals (*first panel*), we infer that the trapping efficiency of a clean foil would have varied from 0.3 in January to approximately 0.1 toward the end of the exposure period in May (*second panel*). Considering the fact that the trapping efficiencies of the foils had degraded at the end of the exposure (see Table 1), we assume trapping efficiencies as delineated by the dashed line in the second panel of Figure 9. The survival probability against ionization of interstellar neutrals arriving at the collector varied from 0.47 at the beginning of the exposure period to 0.67 at its end (*third panel*). Combining these values, interpolating the trapping efficiencies before and after exposure (given in Table 1), and taking into account the focusing of interstellar helium due to solar gravitation in the innermost heliosphere (*fourth panel*) results in an estimate of the LISM helium density of  $0.01 \text{ cm}^{-3}$ , using our value of  $1.0 \times 10^9$  collected  $^4\text{He}$  particles per  $\text{cm}^2$ . This value is more or less consistent with the values obtained from the *Ulysses*/GAS experiment (Witte et al. 1996) and from pick-up ion measurements obtained by other authors

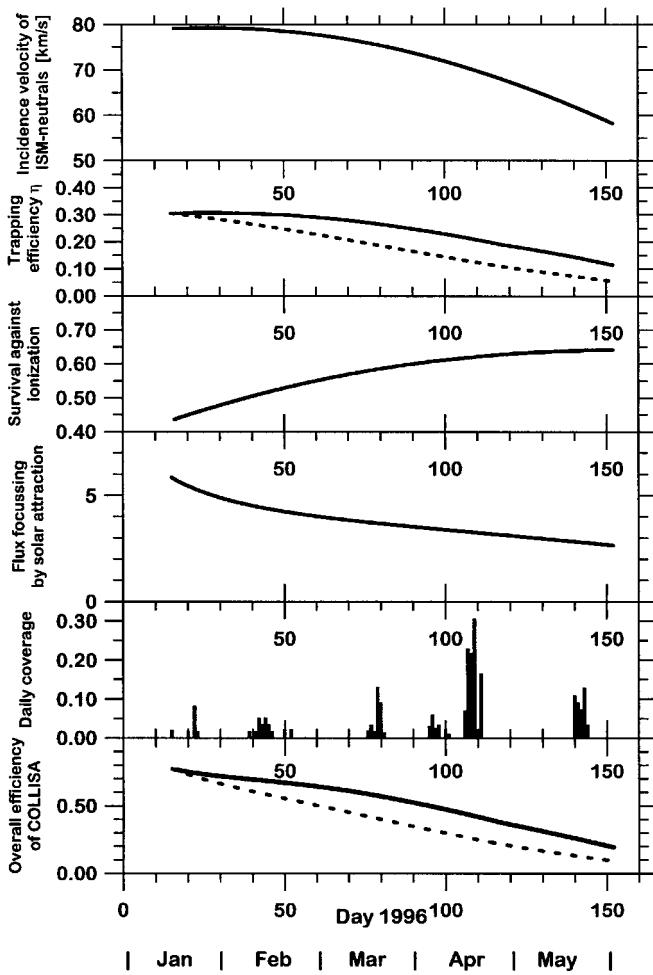


FIG. 9.—Derivation of the neutral helium flux outside the heliosphere from the observed flux at 1 AU. The seasonal variation of the relative speed (Earth-interstellar neutrals) is shown in the topmost panel. Depending on the relative speed, the trapping efficiency in the foils changes (*second panel*). The dashed line illustrates an interpolated curve for effective trapping efficiencies, taking into account the apparent degradation of trapping properties, possibly caused by surface contaminants. The third panel illustrates the fraction of neutral helium surviving against ionization by solar EUV up to the trapping site. The fourth panel shows the effect of gravitational focusing by the Sun. The fifth panel illustrates the daily exposure coverage, and the sixth panel gives the overall efficiency of COLLISA for clean (*solid line*) and degraded foils (*dashed line*).

(Gloeckler 1996; Geiss & Witte 1996; Möbius 1996). Note that the *ratio* of trapping efficiencies,  $\eta_3/\eta_4$  (see Table 1), showed no modification during exposure. Hence, the parameters used for the determination of the interstellar isotopic helium ratio are not affected by the deterioration of the exposed foils.

7.2. Interstellar  $^3\text{He}/^4\text{He}$  from COLLISA: Comparison with Other Galactic Samples

Knowledge of the helium isotopic ratio in different locations of the Galaxy is necessary to test the predictions of Galactic chemical evolution models (GCE) and to constrain their input parameters. In particular, the determination of the  $^3\text{He}$  abundance can have important consequences for stellar evolution models. According to the standard theory of stellar  $^3\text{He}$  nucleosynthesis, solar-type stars are net producers of  $^3\text{He}$  (Palla & Stahler 1991, 1993). As a conse-

quence, the Galactic  $^3\text{He}/\text{H}$  ratio should grow with time and should be higher in the inner region of the Galaxy, where stellar processing has been more active. The ratio observed in protosolar objects, such as meteorites or Jupiter’s atmosphere, should therefore be significantly lower than the ratio presently observed in the interstellar medium.

So far there has been no clear evidence for such a trend. Observations of astrophysical objects with different Galactic ages have all shown a  $^3\text{He}/\text{H}$  ratio ranging from 1.5 to  $1.6 \times 10^{-5}$  (equivalent to a  $^3\text{He}/^4\text{He}$  ratio of  $1.5\text{--}1.6 \times 10^{-4}$  if the standard helium abundance  $^4\text{He}/\text{H} = 0.10$  is used). Our value is consistent with this result.

Table 5 shows the results of some of the most recent outcomes about the helium isotopic ratio in different objects.

The helium isotopic ratio in the LISM derived from direct collection of neutral interstellar matter is, within the large given error bars, somewhat lower than the ratio derived from measurements of pickup ions. A few additional comments to Table 5 are appropriate. The helium isotopic abundance ratio in the solar outer convective zone inferred from solar wind measurements cannot be directly compared to an ancient ambient interstellar gas value since it represents the protosolar  $^3\text{He}+\text{D}$  abundance (Geiss et al. 1972), slightly increased by a few percent because of different secular gravitational settling of  $^3\text{He}$  and  $^4\text{He}$  into the radiative zone (Gautier & Morel 1997) and some possible internal turbulent mixing (Bochsler, Geiss, & Maeder 1990).

Lellouch et al. (2001), using data from the Short-Wavelength Spectrometer on board the *Infrared Space Observatory*, derived a protosolar deuterium abundance in the atmospheres of Jupiter and Saturn of  $(2.1 \pm 0.4) \times 10^{-5}$  and  $(1.7^{+0.75}_{-0.45}) \times 10^{-5}$ , respectively. Thus the best estimate of  $^3\text{He}/\text{H}$ , inferred from solar observations, ranges from 1.4 to  $1.8 \times 10^{-5}$  (see also Mahaffy et al. 1998; Geiss 1993). A somewhat lower value, which is possibly also representative for the isotopic ratio  $^3\text{He}/^4\text{He}$  in the protosolar cloud, has recently been found in the so-called phase Q of meteorites (Busemann, Baur, & Wieler 2001). This is another meteoritic component, which exhibits noble gas isotopic ratios close to solar values. The  $^3\text{He}/^4\text{He}$  ratio of phase Q can therefore be used to derive an independent protosolar  $^3\text{He}/\text{H}$  value and to compare it with observations on other meteorites and with the value derived from Jupiter’s atmosphere.

TABLE 5  
OBSERVED  $^3\text{He}/^4\text{He}$  RATIOS.

Sample	Value ( $\times 10^{-4}$ )	Reference
LISM (neutrals) .....	$1.7 \pm 0.8$	1
LISM (pickup ions).....	$2.48^{+0.68}_{-0.62}$	2
Meteorites (presolar grains) .....	$1.5 \pm 0.3$	3
Meteorites (phase Q).....	$1.23 \pm 0.02$	4
Jupiter atmosphere .....	$1.66 \pm 0.05$	5
H II regions.....	$1.50 \pm 0.58$	6
Sun (outer convective zone).....	$3.7 \pm 0.7$	7

REFERENCES.—(1) This work; (2) Gloeckler & Geiss 1998; (3) Geiss 1993; (4) Busemann et al. 2001; (5) Mahaffy et al. 1998; (6) derived from  $^3\text{He}/\text{H}$  given by Bania et al. 2000 and using  $^4\text{He}/\text{H} = 0.1$ ; (7) Bodmer & Bochsler 1998, in agreement with Gloeckler & Geiss 1998.

The present-day LISM ratio obtained with the COLLISA experiment is consistent with the value derived from  $^3\text{He}/\text{H}$  observations in H II regions, and it is also consistent with the protosolar ratios observed in meteorites and in Jupiter's atmosphere. Considering all the evidence given in Table 5, we conclude that the small remaining difference between the abundance of  $^3\text{He}$  observed in the present-day LISM and the abundances inferred from "older" objects (i.e., from the atmosphere of Jupiter and from meteorites) is insignificant.

### 7.3. Implications for GCE Models: the " $^3\text{He}$ Problem"

The value of the helium isotopic ratio in the LISM presented above confirms that no substantial  $^3\text{He}$  enrichment occurred in the Galaxy, at least not during the last 4.5 Gyr. This result contradicts the expectations of conventional stellar evolution models, which predicted the release of great amounts of  $^3\text{He}$  from low-mass stars at the end of their main-sequence phase. The  $^3\text{He}$  abundances predicted by these models differ, in fact, by almost 1 order of magnitude from the abundances observed in both the presolar material and the LISM ( $^3\text{He}/\text{H} \sim 10^{-5}$ ), but on the other hand they agree with observations of a small sample of planetary nebulae ( $^3\text{He}/\text{H} = 2\text{--}5 \times 10^{-4}$ ) (Bania, Rood, & Balser 2000, 2002; Balser et al. 1997). The discrepancy between the observed and the theoretically predicted values could be avoided if "extra-mixing" occurred below the convective zone of low-mass stars ( $\leq 2 M_{\odot}$ ) on the red giant branch (Charbonnel 1995, 1998). This process would in fact be able to destroy  $^3\text{He}$  by transforming it into  $^4\text{He}$  and into heavier elements. However, in order to explain the values observed in planetary nebulae, which indicate that some stars have to be net producers of  $^3\text{He}$ , it has been suggested that extra-mixing does not take place in all low-mass stars before severe mass losses occur. Recently, Chiappini & Matteucci (2000), adopting a new version of their "two-infall" model, have investigated the evolution of  $^3\text{He}$  for different percentages of low-mass stars in which such extra-mixing occurs. They found that the best fit with observations was reached when this mechanism occurs in 93% of the cases. A similar result was found by Tosi (2000). In Figure 10 the mentioned models are compared with the observed  $^3\text{He}$  abundances given in Table 5.

All curves delineate the temporal evolution of the Galactic  $^3\text{He}/\text{H}$  abundance ratio by numbers. Vertical bars represent the observed values. At the time of solar system formation (9.5 Gyr), the given values are those observed in meteorites (Q phase and presolar grains) and in the atmosphere of Jupiter. At 14 Gyr, present-day LISM values derived from neutrals and pickup ion measurements and from observations of H II regions are shown. In the upper part of the figure, the value measured in the planetary nebula NGC 3242 is also shown. Solid lines indicate the prediction of the "Tosi-1" model (Tosi 2000) when 0%, 90%, and 100% of the low-mass stars are supposed to experience extra-mixing. Dashed lines, labeled "CM," show Galactic  $^3\text{He}$  evolution according to the "two-infall" model (Chiappini & Matteucci 2000) for the cases when 0%, 93% and 99% of low-mass stars undergo extra-mixing. As can be seen, the best fit with observational data is obtained by the Tosi-1 model, when 100% of low-mass stars are assumed to experience extra-mixing. Because of instrument sensitivity limitations, the sample of planetary nebulae observed so far has in

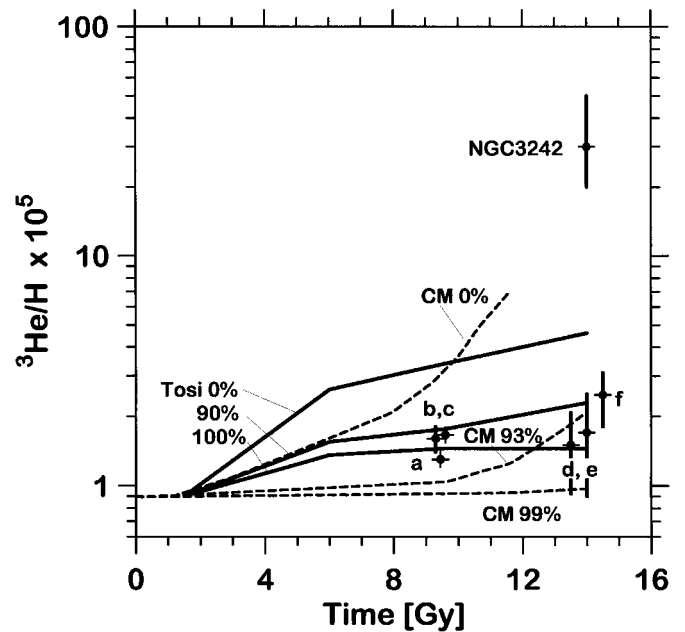


FIG. 10.— $^3\text{He}$  Galactic evolution vs. time according to the Tosi-1 model (Tosi 2000) and the "two-infall" model (Chiappini & Matteucci 2000). Full lines show the results of the Tosi-model with different percentages of "cool bottom processing" to destroy  $^3\text{He}$  in low-mass stars. Dashed curves illustrate the model of Chiappini & Matteucci (2000), again with different percentages of low-mass stars ( $M < 2.5 M_{\odot}$ ), which completely destroy their  $^3\text{He}$ . The symbols at 9.5 and 14 Gyr represent the values derived from observations given by (a) Busemann et al. (2001), (b) Geiss (1993), (c) Mahaffy et al. (1998), (d) Bania et al. (2000), (e) this work, and (f) Gloeckler & Geiss (1998).

fact been chosen in a way to maximize the likelihood of  $^3\text{He}$  detection (Bania et al. 2000). The objects selected belong to the old thick-disk halo population, whose progenitors were probably low-mass stars with a longer main-sequence lifetime and which had therefore an enhanced likelihood of producing great amounts of  $^3\text{He}$ . Planetary nebulae with high  $^3\text{He}$  abundances are apparently not representative ejecta of typical low-mass stars but are extremely peculiar objects.

## 8. CONCLUSIONS

In the framework of the COLLISA project we have determined the helium isotopic ratio in the LISM by applying the foil collection technique. The results have demonstrated the suitability of the foil collection technique for capturing  $^3\text{He}$  and  $^4\text{He}$  particles of interstellar origin in a near-Earth orbit. The ratio derived from the measurements  $^3\text{He}/^4\text{He} = (1.7 \pm 0.8) \times 10^{-4}$  is somewhat lower but still consistent with the LISM value derived from observations of interstellar pickup ions. Our value is in better agreement with  $^3\text{He}$  abundances observed in protosolar material and H II regions. The result confirms the hypothesis that no significant enrichment of  $^3\text{He}$  occurred in the Galaxy during the last 4.5 Gyr. The comparison between the COLLISA interstellar ratio and some GCE theoretical predictions suggests that the amount of stars in which extra-mixing occurs could be even larger than what was expected. It confirms the discrepancy with the  $^3\text{He}$  abundance in planetary nebulae, which has been attributed to the biased selection of the objects observed so far (Bania et al. 2002).

A few more samples of foils exposed to the interstellar inflow are available, and their mass spectrometric analysis is in preparation.

The authors would like to express our gratitude to all participants in the COLLISA experiment, especially V. Karrask of the Energia Corporation, the Khrunichev Center, and to the COLLISA team members V. Chernov, E. Gevorkova, V. V. Krapchenkov, and A. V. Prudkoglyad of the Space Research Institute of the

Russian Academy of Sciences. We are specially grateful to the cosmonauts Sergey Avdeev, Thomas Reiter, Yury Onufrienko, and Yury Usachev for exchanging our cassettes in space. Thanks are due to O. Eugster and P. Eberhardt for many useful discussions, to J. Fischer for his support during the construction phase of the experiment, and to A. Schaller and to A. Etter for their technical support. We acknowledge the help of an anonymous referee who contributed numerous critical comments. This work was supported by the Swiss National Science Foundation.

## REFERENCES

- Balsler, D. S., Bania, T. M., Rood, R. T., & Wilson, T. L. 1997, *ApJ*, 483, 320
- Bania, T. M., Rood, R. T., & Balsler, D. S. 2000, in *IAU Symp. 198, The Light Elements and Their Evolution*, ed. L. da Silva, M. Spite, & J. R. de Medeiros (Provo: ASP), 214
- . 2002, *Nature*, 415, 54
- Bassi, M. L. 1997, Ph.D. thesis, Univ. Bern
- Bochsler, P., Geiss, P., & Maeder, A. 1990, *Sol. Phys.*, 128, 203
- Bodmer, R., & Bochler, P. 1998, *A&A*, 337, 921
- Bühler, F., et al. 2000, *Ap&SS*, 274, 19
- Busemann, H., Baur, H., & Wieler, R. 2001, *Lunar Planet. Sci. Conf. 32, Abstract8* (CD-ROM; Houston: LPI)
- Charbonnel, C. 1995, *ApJ*, 453, L41
- . 1998, *Space Sci. Rev.*, 84, 199
- Chassefière, E., Bertaux, J. J., Lallement, R., & Kurt, V. G. 1986, *A&A*, 160, 229
- Chassefière, E., Dalaudier, F., & Bertaux, J. L. 1988, *A&A*, 201, 113
- Chiappini, C., & Matteucci, F. 2000, in *IAU Symp. 198, The Light Elements and Their Evolution*, ed. L. da Silva, M. Spite, & J. R. de Medeiros (Provo: ASP), 540
- Filleux, C., Mörgeli, M., Stettler, W., Eberhardt, P., & Geiss, J. 1980, *Radiat. Effects*, 46, 1
- Galli, D., Palla, F., Ferrini, F., & Penco, U. 1995, *ApJ*, 443, 536
- Galli, D., Stanghellini, L., Tosi, M., & Palla, F. 1997, *ApJ*, 477, 218
- Gautier, D., & Morel, P. 1997, *A&A*, 323, L9
- Geiss, J. 1993, in *Origin and Evolution of the Elements*, ed. N. Prantzos, E. Vangioni-Flam, & M. Cassè (Cambridge: Cambridge Univ. Press), 89
- Geiss, J., Bühler, F., Cerutti, H., Eberhardt, P., & Filleux, Ch. 1972, *Apollo 16 Preliminary Science Report* (NASA SP-315), Chap. 14
- Geiss, J., Eberhardt, P., Bühler, F., Meister, J., & Signer, P. 1970, *J. Geophys. Res.*, 75, 5972
- Geiss, J., & Witte, M. 1996, *Space Sci. Rev.*, 78, 229
- Ghielmetti, A. G., Balsiger, H., Bänninger, R., Eberhardt, P., Geiss, J., & Young, D. T. 1983, *Rev. Sci. Instrum.*, 54, 425
- Gloeckler, G. 1996, *Space Sci. Rev.*, 87, 335
- Gloeckler, G., & Geiss, J. 1998, *Space Sci. Rev.*, 84, 275
- Jordi, M. 1982, M.S. thesis, Univ. Bern
- . 1986, Ph.D. thesis, Univ. Bern
- Lellouch, E., Bézard, B., Fouchet, T., Feuchtgruber, H., Encrenaz, T., & Graauw, T. 2001, *A&A*, 370, 610
- Mahaffy, P. R., Donahue, T. M., Atreya, S. K., Owen, T. C., & Niemann, H. B. 1998, *Space Sci. Rev.*, 84, 251
- Möbius, E. 1996, *Space Sci. Rev.*, 78, 375
- Olive, K. A., Steigman, G., & Walker, T. P. 2000, *Phys. Rep.*, 333, 389
- Palla, F., & Stahler, S. W. 1991, *ApJ*, 375, 288
- . 1993, *ApJ*, 418, 414
- Rood, R. T., Bania, T. M., Balsler, D. S., & Wilson, T. L. 1998, *Space Sci. Rev.*, 84, 185
- Sakar, S. 1996, *Rep. Prog. Phys.*, 59, 1493
- Schramm, D. N., & Turner, M. S. 1998, *Rev. Mod. Phys.*, 70, 303
- Steigman, G. 1994, *The Light-Element Abundances*, ed. P. Crain (Berlin: Springer), 10
- Tosi, M. 2000, in *IAU Symp. 198, The Light Elements and Their Evolution*, ed. L. da Silva, M. Spite, & J. R. de Medeiros (Provo: ASP), 525
- Witte, M., Banaszkiewicz, M., & Rosenbauer, H. 1996, *Space Sci. Rev.*, 78, 289
- Zastenker, G. N., et al. 2002, *Cosmic Res.*, 40, 347
- Ziegler J. F., Biersack, J. P., & Littmark, U. 1985, *The Stopping and Range of Ions in Solids* (Tarrytown: Pergamon)